PAPER REF: 4644

STRESS INTENSITY FACTOR COMPUTATION: EXTENDED FINITE ELEMENT METHOD (X-FEM) APPLIED TO 3D ENGINEERING PROBLEMS

A. Luís da Silva[1,2*] Hubert Maigre[3], Anthony Gravouil[3], Abílio M.P. de Jesus[2,4], António A. Fernandes[1,2]
[1]Faculty of Engineering of University of Porto (FEUP), Portugal
[2]Institute of Mechanical Engineering (IDMEC), University of Porto, Porto, Portugal
[3]National Institute for Applied Sciences (INSA), Lyon, France
[4]Univerity of Trás-os-Montes e Alto Douro (UTAD), Vila Real, Portugal
[(*)]*Email:* a.luis.l.silva@gmail.com

ABSTRACT

This paper presents a numerical study concerning the fatigue modelling of welded specimens made of S355 steel. The welded specimens were inspired by a welded joint of a connection between the diaphragm and a transverse stiffener of the Alcácer do Sal Portuguese railway bridge. The Alcácer do Sal Bridge is a composite bowstring railway bridge, located in the Portuguese railway line. A fatigue experimental campaign of small scale welded specimens was performed using four variations of the welded joint. Numerical models were used to compute the stress intensity factor ranges. The stress intensity factors were computed by means of the contour integral method, using a 3D eXtended Finite Element Method (X-FEM), as well as the Virtual Crack Closure Technique (VCCT) with standard Finite Element Method (FEM). In addition, fatigue lives were computed and compared with available experimental data. Very accurate predictions of the mean S-N curves were derived.

Keywords: EXtended Finite Element Method, Finite Element method, Stress Intensity Factor, Contour Integral, Virtual Crack Closure Technique, Fatigue, Welded Joints.

INTRODUCTION

Solving three-dimensional fracture/fatigue engineering problems by standard finite element methods can be quite a challenge, since the need to generate a suitable mesh which conforms to both the propagating crack surfaces and the surfaces of the component constitutes a cumbersome task. If the crack surface is not aligned with the element boundaries, the displacement discontinuity and the traction conditions on the crack surface cannot be treated as usual in a standard finite element analysis. Furthermore, for standard finite elements, the mesh must be built substantially more refined around the crack than in the remainder of the model (Moës & Belytschko, 2002). The difficulty increases when crack growth modelling is intended, because in this analysis, the finite element mesh must be remeshed in the vicinity of the crack. The eXtended Finite Element Method (X-FEM) (Belytschko & Black, 1999) presents several improvements regarding the numerical crack growth modelling, because no remeshing procedures are required. The concept of the X-FEM approach uses a displacement field approximation, able to model an arbitrary discontinuity and the near-tip asymptotic crack fields (Moës & Belytschko, 2002). The methodology was first presented by Belytschko (Belytschko & Black, 1999) and Moës (Moës *et al.*, 1999). Finite element, with additional enriched functions, coupled to the partition of unity concept, introduced by Babuška and Melenk (1997), are used. The resulting approximation can be used to treat cracks that are arbitrarily aligned in the finite element mesh with great accuracy.

This paper presents a numerical study, the main goal is to model welded joints made of S355 steel using both ANSYS and ABAQUS codes. The modelled welded joints were inspired from a welded joint of an actual connection between a diaphragm and a transverse stiffener of the Portuguese Alcácer do Sal railway bridge. An experimental campaign of fatigue tests of small-scale welded specimens is performed. Several geometric parameters were investigated, namely the welded configuration and the plate thickness, where fatigue cracks are expected to propagate. Numerical models were used to assess the stress intensity factor range. Contour integral method using a 3D X-FEM (ABAQUS approach), as well as the virtual crack closure technique (VCCT), as described by Krueger (Krueger, 2004), with standard FEM (ANSYS approach) was considered. The fatigue crack growth was modelled using Linear Elastic Fracture Mechanics (LEFM) and the Paris Law. Crack initiation was also accounted by means of a local notch approach. Fatigue lives were compared to available experimental data.

ALCÁCER DO SAL BRIDGE AND WELDED DETAILS

The Alcácer do Sal Bridge (Fig. 1) is a composite bowstring railway bridge, located in the Portuguese railway line that links Lisbon to Algarve. Its construction occurred from 2007 to 2010. The bridge has 3 spans of 160 m, a total length of 480 m and is part of a longer structure composed by the North access viaduct (with a length of 1115 m), the Bridge and the South access viaduct (with a length of 1140 m). The bridge's deck is suspended axially by 18 vertical hangers per arch, with the hangers being placed 8 m apart from each other.

Fig.1 Alcácer do Sal Bridge.

The cross section of the deck is a composite box-girder, with 15.85 m width and about 3 m height. The steel box has a total height of 2.6 m and the concrete slab has a total thickness of 0.40 m to 0.20 m. A diaphragm is present at each deck to hanger connection section, with the corresponding 18 diaphragms per span. Transversal stiffeners are placed at the bottom flange, half-way between diaphragms.

Figure 2 and 3 show the welded specimens, which were modelled using finite elements. A total of four welded joints were modelled: one welded specimen with the same weld configuration of the bridge detail and a thickness of 5 mm (W1 series) (Fig. 3a)); one welded specimen with a weld configuration according to EC3 and a thickness of 5 mm (W2 series) (Fig. 3b)); one welded specimen with the same weld configuration of the bridge detail and a thickness of 12 mm (W3 series) (Fig. 3c)) and one welded specimen with a weld configuration according to EC3 and a thickness of 12 mm (W4 series) (Fig. 3d)).

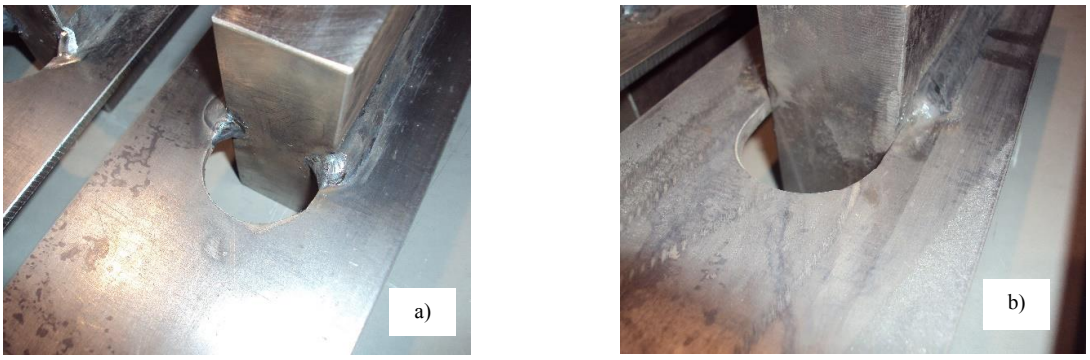

Figure 2. Welded joint details: a) fillet weld according bridge detail; b) fillet weld according EC3.

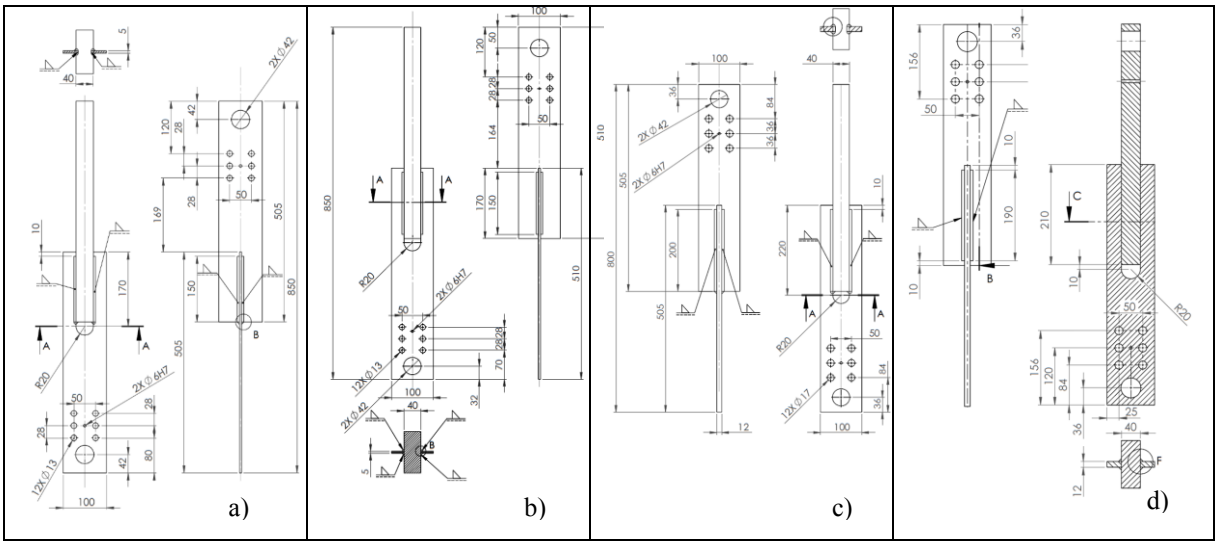

Figure 3. Welded specimens geometry: a) welded specimens with the same weld configuration of the bridge detail and a thickness of 5 mm (W1 series); b) welded specimens with a weld configuration according to EC3 and a thickness of 5 mm (W2 series); c) welded specimens with the same weld configuration of the bridge detail and a thickness of 12 mm (W3 series); d) welded specimens with a weld configuration according to EC3 and a thickness of 12 mm (W4 series).

FATIGUE MODELLING

In order to assess numerical S-N curves of welded joints, finite element models of welded specimens were created. Figures 4 and 5 show a numerical analysis of the welded joints performed using two procedures: standard FEM (Fig. 4) and XFEM (Fig. 5). Fatigue life predictions were assessed including both fatigue crack initiation and fatigue crack propagation phases. The number of cycles to initiate a fatigue crack was computed using local notch strain approaches. The required elastoplastic strains were computed using the Neuber (Neuber, 1961) and Ramberg-Osgood (Ramberg and Osgood, 1943) relations:

$$\begin{cases} \dfrac{(k_t \Delta\sigma_{nom})^2}{E} = \dfrac{\Delta\sigma_{loc}{}^2}{E} + 2\Delta\sigma_{LOC}\left(\dfrac{\Delta\sigma_{loc}}{2K'}\right)^{1/n'} \\ \Delta\varepsilon_{loc} = \dfrac{\Delta\sigma_{loc}}{E} + 2\left(\dfrac{\Delta\sigma_{loc}}{2K'}\right)^{1/n'} \end{cases} \tag{1}$$

where k_t is the elastic stress concentration factor, K' and n' are, respectively, the cyclic strain hardening coefficient and exponent. $\Delta\sigma_{nom}$ is the nominal stress range computed at the net area near the hot spot. The stress concentration factor was computed using the finite element model of the investigated welded joints. The number of cycles for crack initiation was computed thru the Morrow relationship (Morrow, 1965):

$$\frac{\Delta\varepsilon_{loc}}{2} = \frac{\sigma'_f}{E}(2N_i)^b + \varepsilon'_f(2N_i)^c \tag{2}$$

where $\Delta\varepsilon_{loc}$ is the local elastoplastic strain range; σ'_f and b are, respectively, the cyclic fatigue strength coefficient and exponent; ε'_f and c are, respectively, the fatigue ductility coefficient and exponent; E is the Young modulus. Table 1 presents all fatigue parameters data used in this paper for S355 structural steel (De Jesus *et al.*, 2012).

The number of cycles corresponding to the crack propagation was computed using both standard FEM and X-FEM methods. The crack propagation simulation using standard FEM can be cumbersome. The propagating crack surfaces and the surfaces of the component need a suitable mesh to be able to compute stress intensity factors, which can be problematic to be done in 3D problems. XFEM approach allows the definition of the crack, independently of the finite element mesh.

Table 1. S355 material data

K´ MPa	**n´**	**σf´** MPa	**b**	**εf´**	**c**
598.85	0.0757	952.2	-0.089	0.7371	-0.664

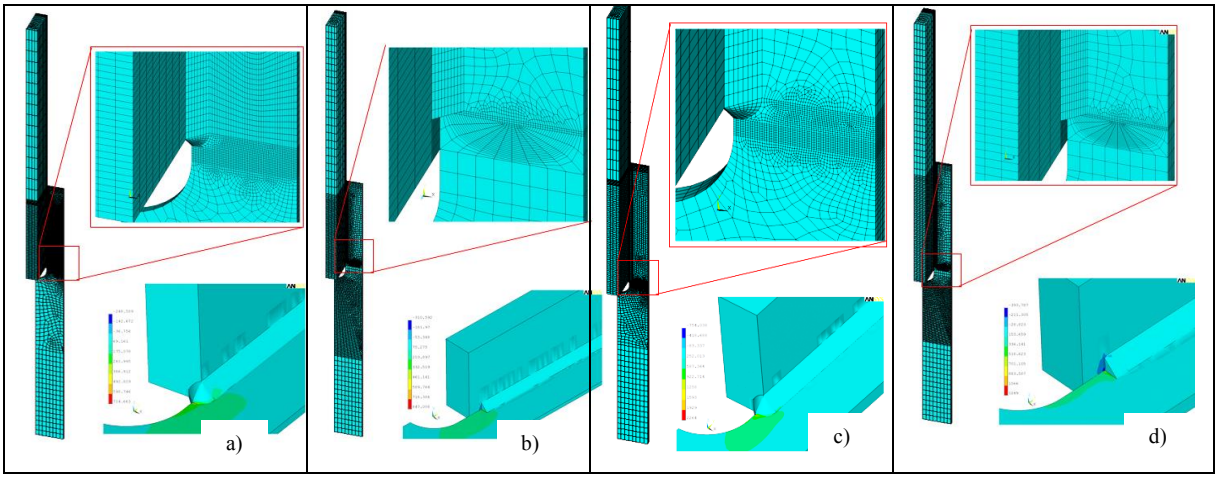

Figure 4. FE models of Welded series obtained using and stress distributions ANSYS: a) W1 series; b) W2 series; c) W3 series; W4 series.

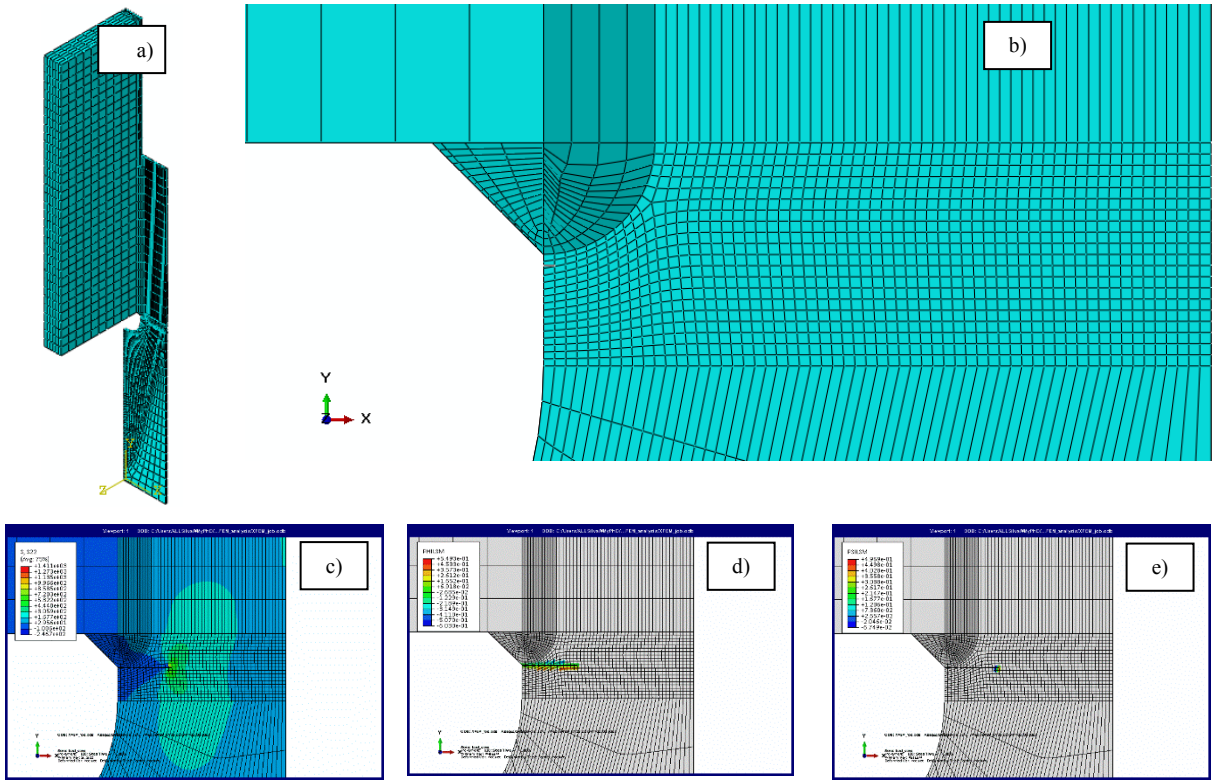

Figure 5. W1 welded specimen modelled using 3D X-FEM: a) global view of the welded specimen finite element mesh; b) detail of the enriched finite elements; c) σ_{yy} stress field maps; d) phi level set function; e) psi level set function.

Concerning the standard FE models, performed in ANSYS, only ¼ of specimens geometries were modelled, taking into account existing symmetries. Figure 4 presents the finite element mesh modelled for all four welded specimens. Materials were considered linear elastic and isotropic (E=210 GPa; ν=0.27). Hexahedral 20 node finite elements were used. The crack path was defined during the finite element mesh generation. Both the initial crack length and the crack increments were define as 0.5mm. Stress intensity factor ranges were compute using the Virtual Crack Closure Technique, as proposed by Krugger (2004). The loading conditions results in dominant pure mode I, which means that only stress intensity for mode I were computed at the crack tip. Figure 4 shows the finite element mesh used to model W1 welded specimens (Figure 4 a)), W2 welded specimens (Figure 4 b)), W3 welded specimens (Figure 4 c)) and W4 welded specimens (Figure 4 d)). Figure 4 also exhibits σ_y (y=loading direction) stress fields.

The X-FEM is a methodology that was incorporated in the finite elements software ABAQUS, which allows the fatigue crack modelling independently of the finite element mesh, enriching all elements cut by the crack, using enrichment functions satisfying the discontinuous behaviour and additional nodal degrees of freedom. The approximation to a displacement field function with the partition of unity enrichment is:

$$\{u\} = \sum_{I=1}^{N} N_I(x)[\{u_I\} + H(x)\{a_I\} + \sum_{\alpha=1}^{4} F_\alpha(x)\{b_I^\alpha\}] \tag{3}$$

where $N_I(x)$ are the usual nodal shape functions; the first term on the right-hand side of the above equation, $\{u_I\}$, is the usual nodal displacement vector associated with the continuous part of the finite element solution; the second term is the product of the nodal enriched degree of freedom vector, $\{a_I\}$, and the associated discontinuous jump function $H(x)$ across the crack surfaces; and the third term is the product of the nodal enriched degree of freedom vector, $\{b_I^{\alpha}\}$, and the associated elastic asymptotic crack-tip functions, $F_{\alpha}(x)$. The first term on the right-hand side is applicable to all the nodes in the model; the second term is valid for nodes whose shape function support is cut by the crack; and the third term is used only for nodes whose shape function support is cut by the crack tip.

A key development that facilitates treatment of cracks in an extended finite element analysis is the description of crack geometry, because the mesh is not required to conform to the crack geometry. The level set method, which is a powerful numerical technique for analyzing and computing interface motion, fits naturally with the extended finite element method and makes it possible to model arbitrary crack growth without remeshing. The crack geometry is defined by two almost-orthogonal signed distance functions. The levels set function ϕ, describes the crack surface, while the second level set function, φ, is used to construct an orthogonal surface so that the intersection of the two surfaces gives the crack front. Finite element models were modelled using ABAQUS code. As referred for FEM analysis, only ¼ of specimens geometries were modelled. Linear hexahedral 8 nodes finite elements were used. Finite elements formulation with reduce integration method was considered.

Figure 5 presents the finite element model of the W1 welded specimen. Finite element mesh used may be observed in Figures 5 a) and b). Figure 5b) shows the mesh region where finite elements were enriched with additional degrees of freedom. Figure 5c) plots the σ_y stress field at the fatigue crack domain. Figures 5 d) and f) exhibit the ϕ and φ level set functions plotted by ABAQUS. Stress intensity factors were computed using the contour integral method available in ABAQUS. In order to evaluate accurately stress intensity factor, several contours were used, as illustrated in Figure 6. As first approach, five contours around the crack tip element were used to compute the stress intensity factors. The second approach to assess the stress intensity factors did not consider contour 1, and the third approach only used contours 3, 4 and 5 to compute stress intensity factors. In order to compute accurate stress intensity factors, the initial crack was considered long enough to assure that the contour box was distant from the plate edge. Although dominant mode I, for the proposed crack growth analysis, both K_1 and K_2 were computed. Therefore, a crack branching procedure was considered (Erdogan and Sih, 1963). The new crack increment angle was computed using the maximum hoop stress criteria:

$$\theta = \arcsin\left(\frac{K_{II}}{\sqrt{K_I^{\,2} + 9K_{II}^{\,2}}}\right) + arctg\left(\frac{3K_{II}}{K_I}\right) \tag{4}$$

An equivalent stress intensity stress is computed using the following relation:

$$K_{eq} = K_I \frac{3\cos\left(\frac{\theta}{2}\right) + \cos\left(\frac{3\theta}{2}\right)}{4} + K_{II} \frac{-3\sin\left(\frac{\theta}{2}\right) - 3\sin\left(\frac{3\theta}{2}\right)}{4} \quad (5)$$

Finally, the number of cycles corresponding to the crack propagation is computed using the Paris' law (Paris and Erdogan, 1963).

RESULTS AND DISCUSSION

Stress intensity factors (SIF) range computed using FEM with VCCT and X-FEM with Contour Integral, for W1, W2, W3 and W4 welded specimens, are plotted, respectively, in Figures 7a), b), c) and d). Figure 7a) presents the stress intensity factors computed for W1 welded specimens loaded to 50kN. Figure 7b) exhibits the stress intensity factors computed for a crack propagating in W2 welded specimens, loaded at 25kN. Figure 7c) shows the stress intensity factors resulting from a crack propagating at the W3 welded specimens, loaded by 50kN load, and the Figure 7d) illustrates the stress intensity factor history computed for a crack growing for W4 welded specimens, loaded by a 75kN load. The red curve corresponds to a numerical SIF results assessed using the ANSYS code combined to the VCCT algorithm, and the other curves were assessed by means of the X-FEM method and the contour integral method, computed using several number of contours. The maximum crack was defined by the maximum stress intensity factor observed in a da/dN compact tension tests, tested for the same stress ratio (De Jesus *et al.*, 2012). The analysis of Figure 7 reveals that the FEM procedure results in higher stress intensity factors, than the X-FEM procedure. Consequently, Figure 7 illustrates that SIF values resulting from FEM analysis, reaches the values for lower crack sizes than resulted from X-FEM analysis. It is important to refer that the finite element mesh used in FEM analysis was coarser than X-FEM models, which may imply higher stress intensity values, and then higher crack propagation rates. Stress intensity factors computed using distinct contours are also plot in Figure 7. The curve resulting from the analysis using all contours around the crack tip element presents some fluctuations. However, once excluded contour 1, the stress intensity results are smooth and convergent.

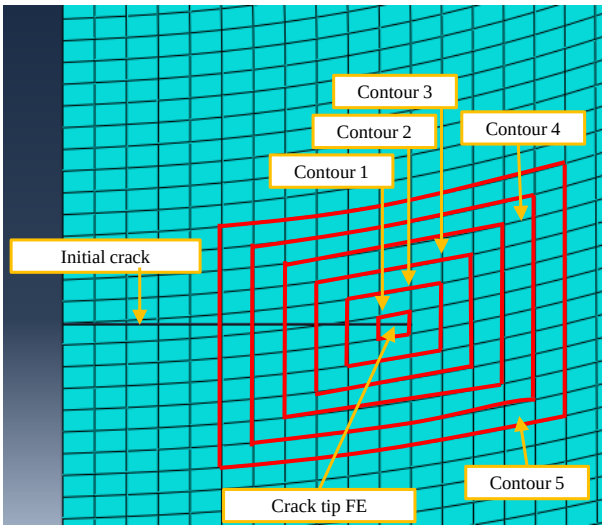

Figure 6. Contours used in the computation of the stress intensity factors with the XFEM approach.

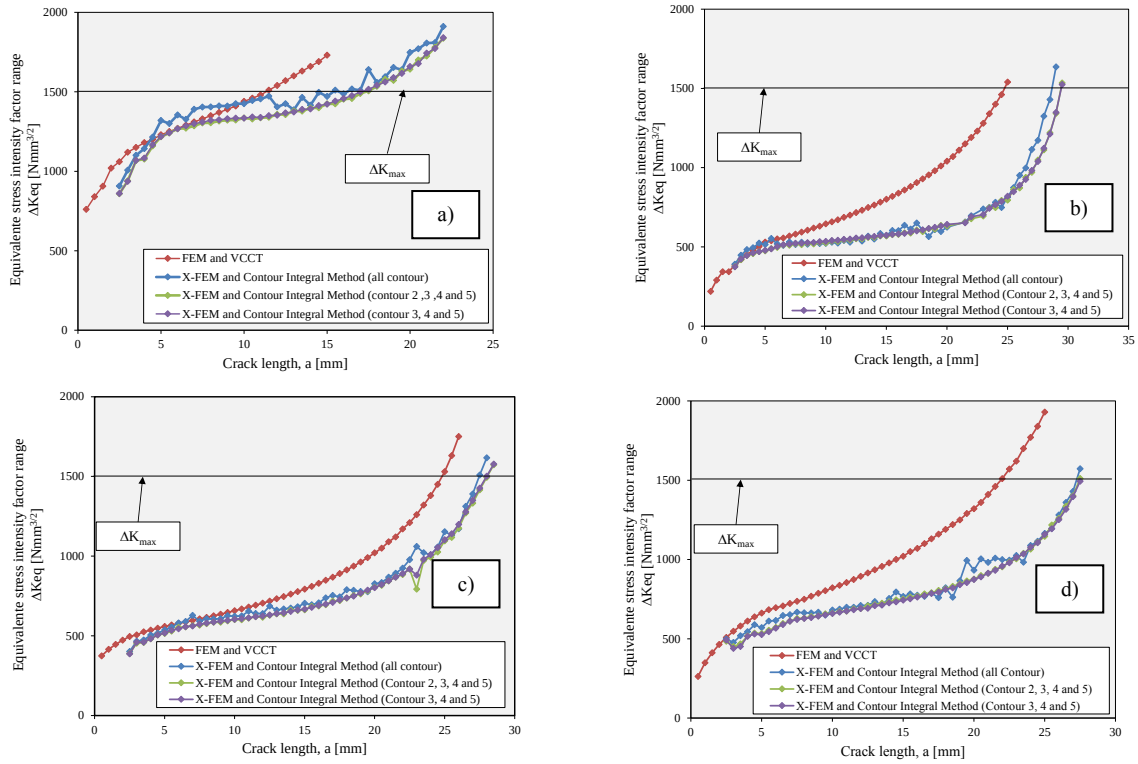

Figure 7. Stress intensity factors range computed using FEM and X-FEM: a) W1 welded specimens loaded at 50kN; b) W2 welded specimens loaded at 25kN; c) W3 welded specimens loaded at 50kN; d) W4 welded specimens loaded at 75kN.

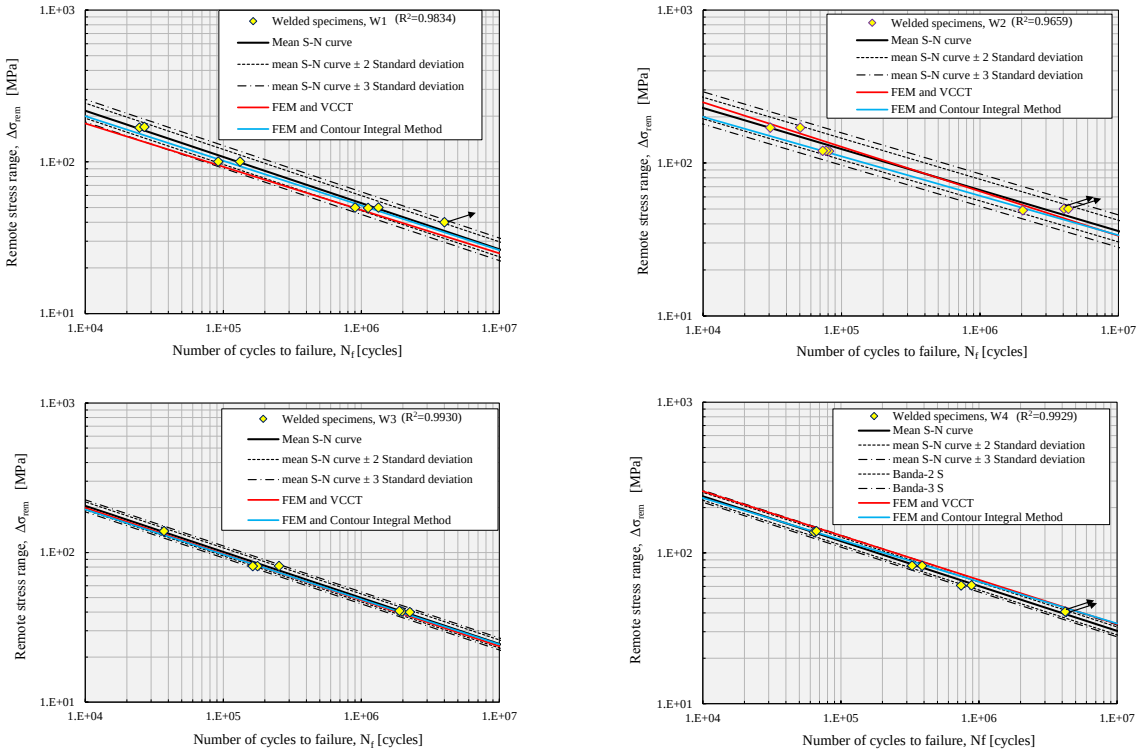

Figure 8. Comparison between experimental S-N data and numerical S-N curves computed using FEM and X-FEM analysis: a) W1 series; b) W2 series; c) W3 series; d) W4 series.

Figure 8 compares the experimental S-N data with numerical S-N curves resulting from crack initiation and propagation modelling, supported by FEM and X-FEM analysis. The analysis of the Figure 8 reveals a very good agreement between the numerical S-N curves and the experimental fatigue data for all welded specimens.

CONCLUSIONS

Numerical S-N curves for four types of welded specimens were computed, taking into account the number of cycles to initiate and propagate fatigue cracks. The number of cycles to initiate a fatigue crack was assessed using a local strain approach. The number of cycles to propagate the crack was computed using the Paris law. The required stress intensity factors were computed based on two alternative techniques. A standard finite element method was considered with the VCCT technique. However, this approach can be complex to apply in 3D problems with complex geometries, once the crack path must be defined according to the finite element mesh. An alternative method to compute the stress intensity factors, using the eXtended finite element method, was adopted. This method allows the fatigue crack modeling, independently of the finite element mesh. Both methods were applied to compute the stress intensity evolution, and some differences were verified in the stress intensity values, required further investigation in order to assess the causes of such discrepancies. The predicted fatigue S-N curves were very consistent with available experimental data, which validates both proposed fatigue model as well as the techniques for stress intensity factors computation.

ACKNOWLEDGMENTS

Authors acknowledge the Fundação para a Ciência e Tecnologia for their financial support through the SFRH/BD/72434/2010 grant.

REFERENCES

Babuška, I., Melenk, J. The Partition of Unity Method. International Journal for Numerical Methods in Engineering, 1997, p. 727-758.

Belytschko, T, Black, T. Elastic crack growth in finite elements with minimal remeshing. International Journal for Numerical Methods in Engineering, 1999, p. 602-620.

de Jesus, A.M.P., Matos, R., Fontoura, B.F.C., Rebelo, C., Simões da Silva, L., Veljkovic, M. A comparison of the fatigue behaviour between S355 and S690 steel grades. Journal of Constructional Steel Research, 2012, p. 140–150.

Erdogan F., Sih, G.C. On the Crack Extension in Plates Under Plane Loading and Transverse Shear. J. Basic Eng. Trans. ASME, 1963, p. 519-527.

Krueger, R. Virtual crack closure technique: History, approach, and applications. Applied Mechanics Reviews. 2004, p. 109-143.

Moës, N., Dolbow, J., Belytschko, T. A finite element method for crack growth without remeshing. International Journal for Numerical Methods in Engineering, 1999, p. 131-150.

Moës, N., Belytschko, T. Extended finite element method for cohesive crack growth. Engineering Fracture Mechanics, 2002, p. 813–833.

Morrow, J. D. Cyclic plastic strain energy and fatigue of metals. Int. Friction, Damping and Cyclic Plasticity, ASTM, STP 378, 1965, p. 45-87.

Neuber, H. Theory of Stress Concentration for Shear-Strain Prismatic Bodies with Arbitrary Nonlinear Stress-Strain Law. Translation of the ASME, Journal of Applied Mechanics. Vol. 28, 1961, p. 544-550.

Paris, P., Erdogan, F. A critical analysis of crack propagation laws. Journal of Basic Engineering. Vol. 85, 1963, p. 528-534.

Ramberg, W., Osgood, W. R. Description of stress-strain curve by three parameters. National Advisory Committee for Aeronautics. Tech. Note No. 902, 1943.